Supporting Information

3D printing lubricative stiff supramolecular polymer hydrogel for meniscus replacement

Chuanchuan Fan, Ziyang Xu, Tengling Wu, Chunyan Cui, Yang Liu, Bo Liu, Jianhai Yang, Wenguang Liu*

School of Materials Science and Engineering, Tianjin Key Laboratory of Composite and Functional Materials,

Tianjin University, Tianjin 300350, China

*Corresponding author (E-mail: wgliu@tju.edu.cn)

EXPERIMENTAL SECTION

Materails. Semicarbazide hydrochloride (98%, Energy Chemical, Shanghai, China), acryloyl chloride (98%, Heowns Company, Tianjin, China), diethyl ether (Yuanli Company, Tianjin, China), 2-hydroxy-2-methyl-1-phenyl-1-propanone (IRGACURE 1173, 98%, Sigma-Aldrich) were used as received. N-acryloylsemicarbazide (NASC) and carboxybetaine acrylamide (CBAA) monomers were synthesized according to the previous work.[1, 2] All other chemicals and solvent were analytical reagents.

Preparation of PNASC-PCBAA-x Gel Systems. A certain mass ratio of NASC and CBAA were dissolved in a mixed solvent of DMSO and H_2O (3/7; v/v), followed by addition of 1 wt% of photoinitiator IRGACURE 1173 (relative to total of NASC and CBAA). The mixture was stirred under N_2 atmosphere until complete dissolution. The mixture was photoinitiatized for 40 min in a UV crosslink oven (XL-1000 UV Crosslinker, Spectronics Corporation, NY, USA). The resultant gels were named as PNASC-PCBAA-x (x is the total concentration of NASC and CBAA, w/v%).

Preparation of PNASC-PCBAA-6-m Hydrogels. A certain mass of NASC and CBAA (NASC/CBAA mass ratio was fixed at 17/3, photoinitiator IRGACURE 1173 was 1 wt%) was loaded into the selected PNASC-PCBAA-6 (NASC: 3.5%, CBAA: 2.5%) thermoreversible gel, which was then heated until a sol state was achieved. The sol was quickly cast into PMMA molds and polymerization was performed for 40 min in a UV crosslink oven. Then the gels were immersed in deionized water to complete solvent exchange, by which the hydrogels were obtained. The resultant hydrogels were coded as PNASC-PCBAA-6-m (m is the total concentration of NASC and CBAA, w/v%)

Measurements of Dynamic Swelling Behaviors and EWCs. The EWCs and swelling behaviors of all the hydrogel sample were measured according to the previous method.[1]

Measurement of Mechanical Properties. The tensile test of hydrogels was carried out on an Instron 2344 Microtester in a water bath at 25 ℃ at a 50 mm min^{-1} stretching rate. Dumbbell shaped hydrogel samples in swelling equilibrium were prepared referring to ATSM standard. In addition, the cylinder-shaped hydrogel samples with diameter of 5 mm and height of 5 mm were used for compressive test at crosshead speed of 10 mm min^{-1}. All the stresses of the hydrogel specimens were acquired by the following formula:

$$\sigma = F/A$$

where F is the applied load and A is the initial cross-sectional area.

For tearing test, two legs of the trouser shaped hydrogel sample are respectively fixed on the base and the crosshead of the tester. The tensile test was performed at a streching rate of 50 mm min^{-1}. The tearing energy was obtained from the following formula:

$$\Gamma = \frac{2Fave}{d}$$

where F_{ave} is the average load during the tear and d is the thickness of samples.

Measurement of Suture Retention Strength. The suture retention strength of cast and printed hydrogels was measured referring to our previous work.[1]

Evaluation of Friction Properties. The friction behavior of hydrogels (cast and printed hydrogels) was tested on a conventional ball-on-disk tribometer to record the friction coefficient at 25 ℃ by using TRB Tribometer (CSM, Switzerland). The contact pair was a stainless steel ball with a diameter of 6 mm and the friction coefficients were calculated by dividing the friction force by the applied normal load according to the system software. The water was chosen as the lubricant for all the tests.

Cell Viability and Evaluation of Cell Adhesion. The assay of cell viability was referred to the reported method.[3] The sterilized hydrogel discs with dimeters of 10 mm were placed into 24-well culture plates, followed by seeding cells with a density of 4×10^4 well onto hydrogel surfaces. The cells were incubated in 5% CO_2 atmosphere at 37 ℃. After culture for 1 and 5 days, the cells in each well were stained for 10 min with 500 μL Calcein AM (2mM), followed by washing twice with PBS and stained for 3 min using EthD-1. Then the cells were observed on an inverted fluorescence microscope (EVOS M5000).

The MTT assays was performed according to the previous work.[4] In detail, Mouse embryo fibroblast (L929) cells with a density of 2×10^4 well were seeded in a 96-well plate. The cells were incubated in 5% CO_2 atmosphere at 37 ℃. After incubating for 24 h, the culture medium was removed, followed by adding 200 μL extraction medium from the hydrogels to each well and further incubated for 24 h. Then, the medium was replaced by growth medium (180 μL) and MTT (20 μL, 5 mg mL^{-1} in PBS) and cultured for additional 4 h in the same condition. Finally, the DMSO (300 μL) was applied to replace the medium and the plate was shaken for 30 min. A ∑960 plate-reader (Meter-tech) was used to measure the optical absorbance of each well at the wavelength of 570 nm. The relative cell viability was calculated by Abs_s / Abs_c × 100%, where Abs_s and Abs_c are the relative fluorescence intensity of the sample and control groups, respectively.

Rheology Test of the Hydrogels and Inks. The dynamic rheology properties of PNASC-PCBAA hydrogels and ink systems were measured by the Anton Paar MCR302 (Austria) with a 25 mm diameter parallel (hydrogels) or taper (inks) plate geometry for all tests. A Peltier device and a solvent trap were respectively used for controlling temperature precisely and retarding the water evaporation during the measuring process. Linear viscoelastic region was defined by carrying out the oscillation amplitude sweep (shear strain: 0.1-1000%, frequency: 1 Hz) to determine an appropriate shear strain to perform oscillatory rheological measurements and finally a 1% shear strain was selected for measuring other rheological properties of hydrogel and inks under the oscillatory mode. The temperature-dependent rheology test with a

temperature range of 25-90 ℃ (heating rate: 5 ℃) and frequency of 1 Hz was performed to characterize the thermoresposive behavior of hydrogels and inks. The steady-state flow tests were carried out to record the variation in viscosity of inks with a shear rate ranging from 1 to 1000 s^{-1} at room temperature. The self-recovery behaviors of inks in response to the shear rate change was evaluated by recording the viscosity changes with the alternate shear rate (shear rate: 1, 200, 400, 800 s^{-1}).

3D Printing of PNAGA-PCBAA-6-40 Hydrogel Scaffolds. Printed hydrogel scaffolds were fabricated by a 3D bioprinter (3D Bio-Architect® Sparrow Regenovo Biotechnology) with a low temperature deposition platform (-5 ℃). CAD/CAM software were used for designing the 3D models and the rabbit's meniscus model was reconstructed from the Micro-CT data via Mimics Research 20.0 software, which used for obtaining the corresponding G-code files through the CuraEngine slice software. The layer-by-layer stack protocol was directed to build up the designed architectures. Then, the homogeneous PNASC-PCBAA-6-m ink was firstly loaded into syringe and successively extruded through the needle under the air pressure of 0.01 MPa at 45 ℃. The printed microfibers were deposited on the glass substance at -5 ℃. Finally, the printed 3D architectures were photo-polymerized for 1 h, and the printed objected were maintained in water for the later testing.

Graft Implantation and Postoperative Observations. All the protocols for the animal experiments were performed according to the guidelines of the Council for the Purpose of Control and Supervision of Experiments on Animals, Government of China. The animal experiments were approved by the Animal Ethical Committee of Tianjin

Institute of Medical and Pharmaceutical Sciences, China (IMPS-EAEP-H-H2021002-01). The adult male rabbits with weight of 2.5-3.0 kg were used for evaluating the performance of the printed PNASC-PCBAA-6-40 hydrogel meniscus scaffolds. The rabbits were anesthetized through an auricular vein injection of sodium pentobarbital solution with a dosage of 35 mg/kg before surgery. Then the rabbits were fixed on the operating table and both hind legs were shaved and disinfected with the iodine. The skin was cut with a bistoury and incising the medial collateral ligament to expose the posterior horn of the medial meniscus. The articular cavity was opened and meniscectomy was carried out by excising the junctures between the posterior/anterior horns of medial meniscus and the tibial plateau in both knee joints. The native (sham) group was the animals with only exposure of the medial meniscus (n = 2 for each time point). Positive control group was the animals(n=3) with meniscus being removed and no hydrogel substitute was implanted. For the experimental group (n=3 for each time point and each type of material), the printed PNASC-PCBAA-6-40 hydrogel meniscus scaffolds and the cast PNASC-30 hydrogel scaffolds were respectively implanted into both knee joints of different rabbits after meniscectomy. The anterior and posterior horns of the meniscus scaffold were respectively sutured to the meniscal capsule and ligament, ensuring that the scaffold was connected to the initial position. Finally, the capsule was closed by nonabsorbable sutures stitching and the rabbits were placed back into the cages to ensure their free moving. Penicillin was intramuscularly injected into the rabbits once daily for 3 days after surgery. The rabbits were then euthanized. Subsequently, their tibia, femur, and the implants were harvested, examined

macroscopically. Then the harvested tissues were fixed with 12% formaldehyde for the histological section staining.

Statistical Analysis. Data are presented as means ± standard deviations. ANOVA was employed to determine whether data groups differed significantly from each other. Statistical significance was defined as having *$P < 0.05$.

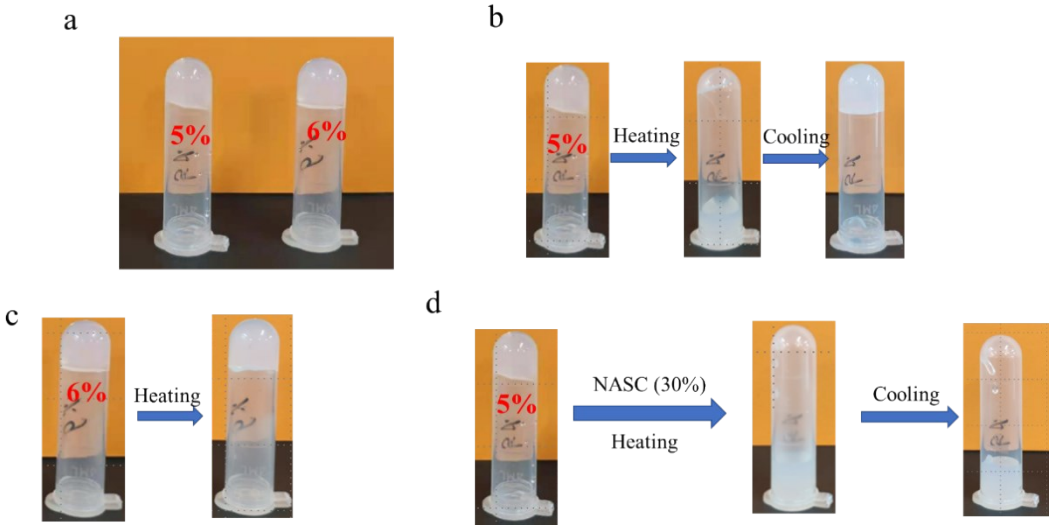

Figure S1. (a) Photographs of PNASC prepared from varied concentrations of monomer (5% and 6%) in a mixed solvent of DMSO/H_2O (7/3; v/v). (b) The state changes of PNASC-5 (the initial monomer concentration is 5%) at a high (95 ℃) and low (25 ℃) temperature. (c) The photographs showing that the PNASC-6 (the initial monomer concentration is 6%) maintained a gel state when the temperature was elevated. (d) The state change of PNASC-5 loading 30% NASC monomer at a high (95 ℃) and low (25 ℃) temperature.

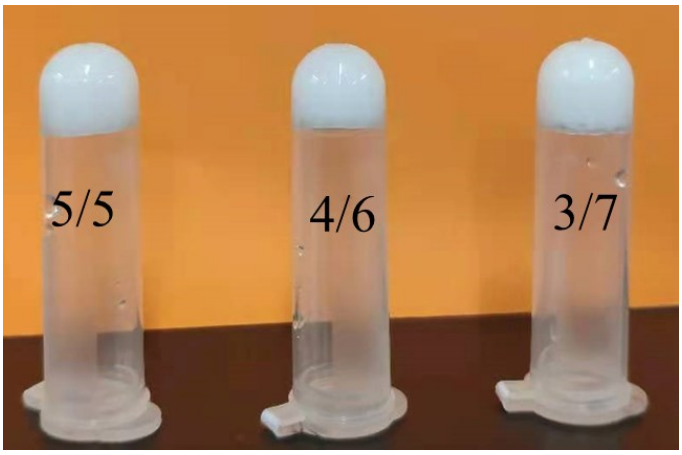

Figure S2. Photographs of PNASC-5 gel prepared from varied volume ratio of DMSO/H_2O (5/5, 4/6, 3/7).

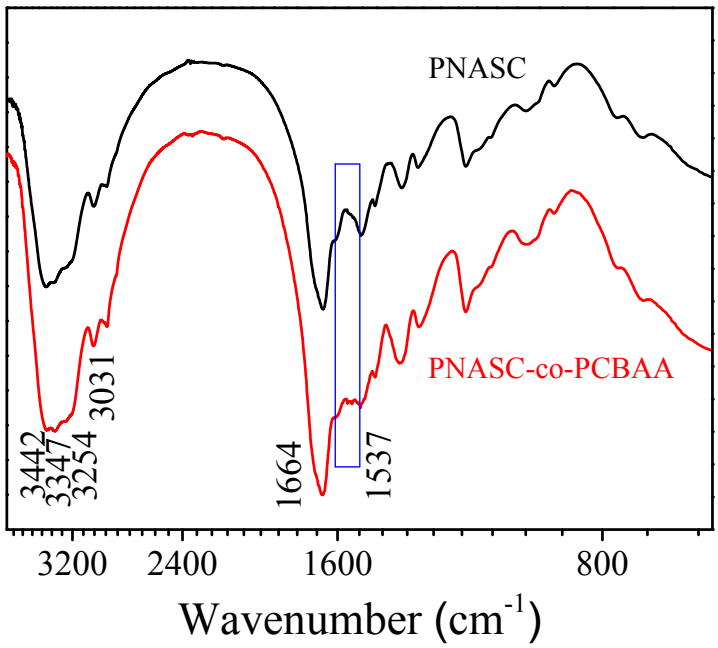

Figure S3. FTIR spectra of PNASC and PNASC-co-PCBAA (NASC/CBAA: 37.5/8.5; m/m). A new peak at 1537 cm^{-1}, corresponding to CH_3-N characteristic peak in CBAA was observed, suggesting the successful incorporation of PCBAA.

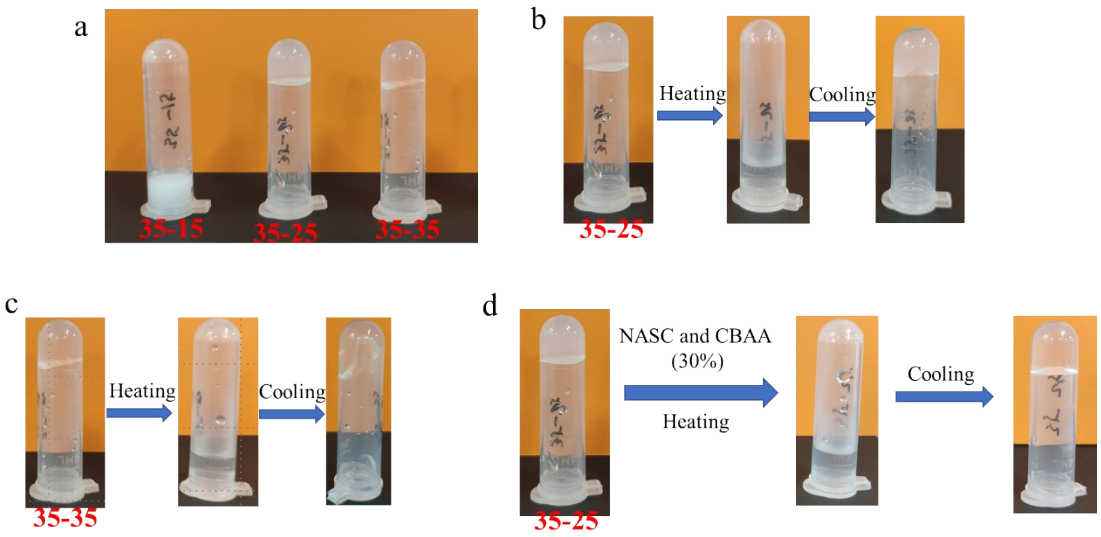

Figure S4. (a) Photographs of PNASC-PCBAA prepared from varied total concentrations of monomer [5%, 35/15 (m/m); 6%, 35/25 (m/m); 7%, 35/35 (m/m)] in a mixed solvent of DMSO/H_2O (3/7; v/v). (b) The state changes of PNASC-PCBAA-6 (the initial NASC/CBAA mass ratio: 35/25) at a high (95 ℃) and low (25 ℃) temperature. (c) The photographs showing that the PNASC-PCBAA-7 gel (the initial NASC/CBAA mass ratio: 35/35) transformed into a sol state when the temperature was elevated and only weaker gel was formed compared to initial gel after the temperature was decreased back to room temperature. (d) The state changes of PNASC-PCBAA-6 loading 30% NASC and CBAA monomer (NASC/CBAA: 17/3; m/m) at a high (95 ℃) and low (25 ℃) temperature.

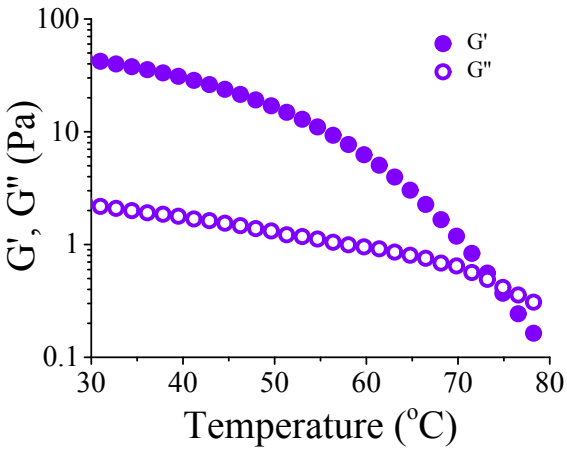

Figure S5. Variation in dynamic storage modulus (G') and loss modulus (G'') of PNASC-PCBAA-6 gel as a function of temperature.

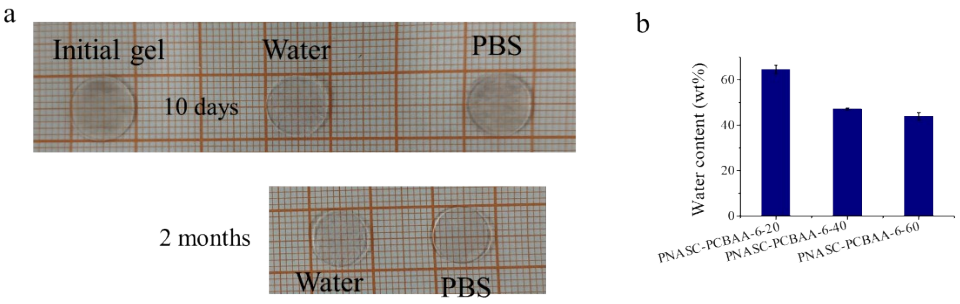

Figure S6. (a) Photos of the PNASC-PCBAA-6-40 gels immersed in water and neutral PBS for 10 days and 2 months; (b) Effect of free monomer concentrations on the EWCs of PNASC-PCBAA-6-m hydrogels. (n=3)

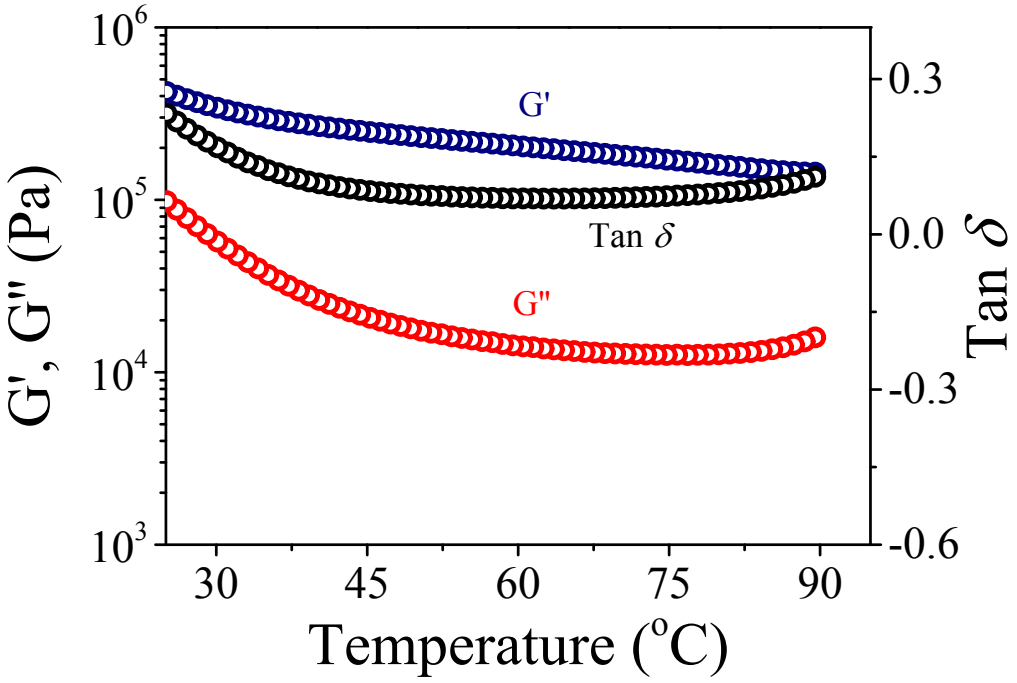

Figure S7. Variation in dynamic storage modulus (G'), loss modulus (G'') and loss factor (tan δ) of PNASC-PCBAA-6-40 hydrogel as a function of temperature.

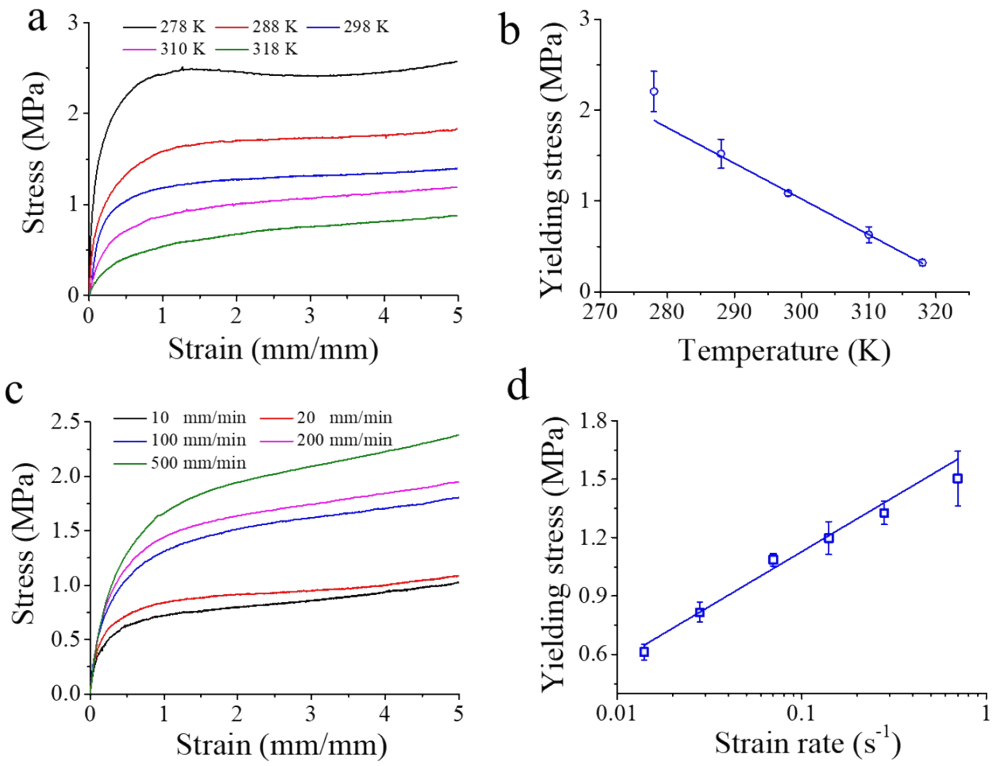

Figure S8. Tensile stress-strain curves of PNASC-PCBAA-6-40 hydrogels determined at different temperatures (a), and different stretching rates (c). Variations of corresponding yielding stress as a function of temperature (b) and strain rate (d). (a) Stretch rate: 50 mm min^{-1}; (c) test temperature: 25 ℃. Error bars represent the standard deviation. (n = 3)

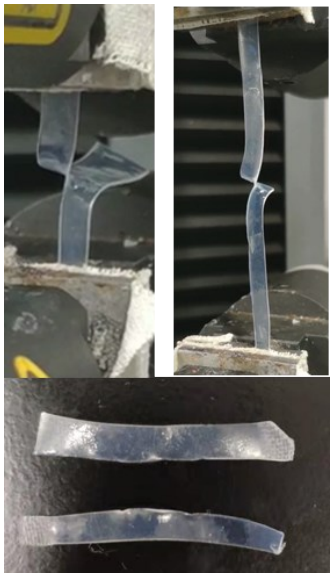

Figure S9. Tearing test of PNASC-PCBAA-6-40 hydrogels.

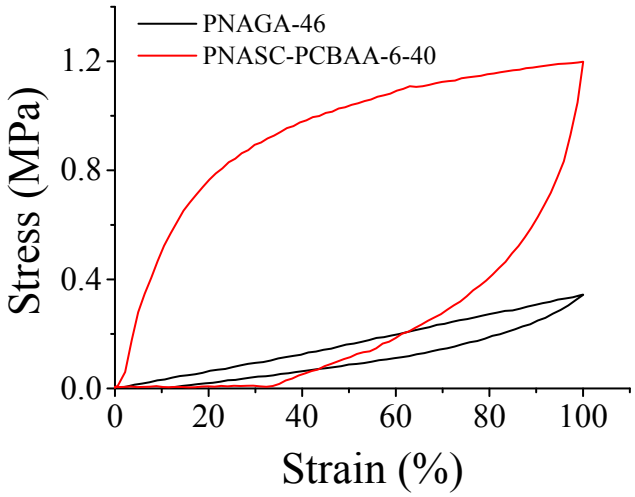

Figure S10. Loading-unloading tests of PNAGA-46 and PNASC-PCBAA-6-40 hydrogels.

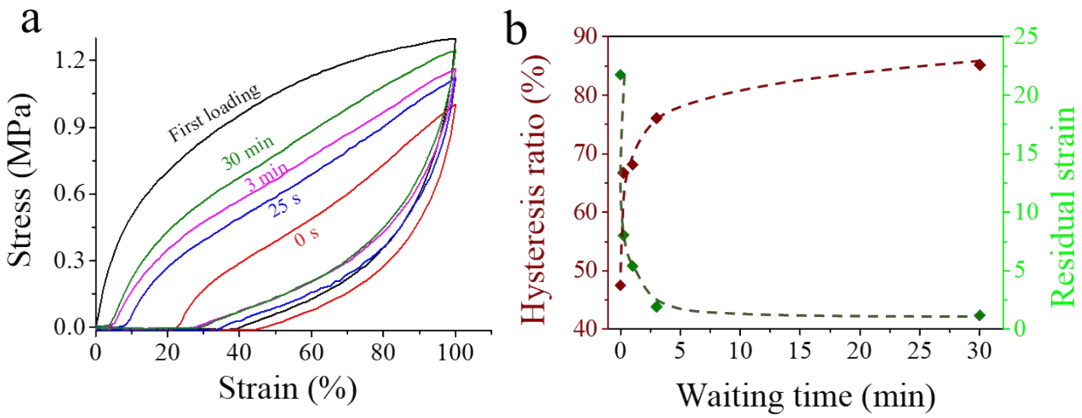

Figure S11. (a) Recovery of PNASC-PCBAA-6-40 hydrogel for different waiting times (0 s, 25 s, 3 min, 30 min) carried out by cyclic tensile tests and (b) waiting time dependent-residual strain and hysteresis ratio (A_2/A_1, A_2 and A_1 are the area of the second and first hysteresis loop, respectively).

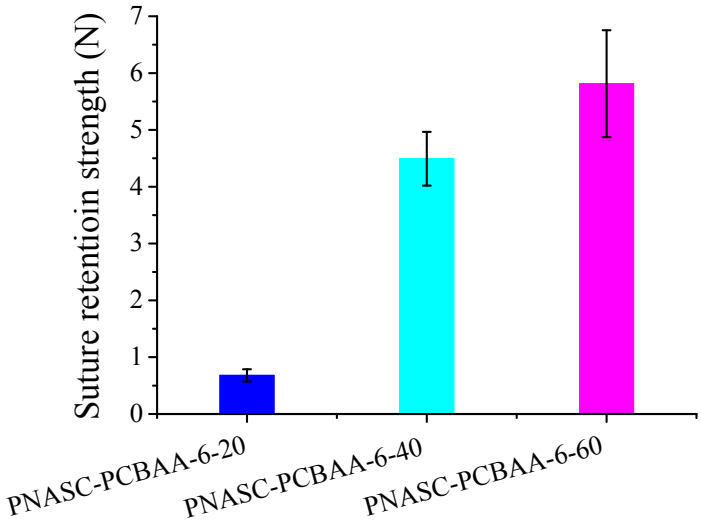

Figure S12. Suture retention strength of PNASC-PCBAA-6-m hydrogels loading different concentrations of free monomers. (n=3)

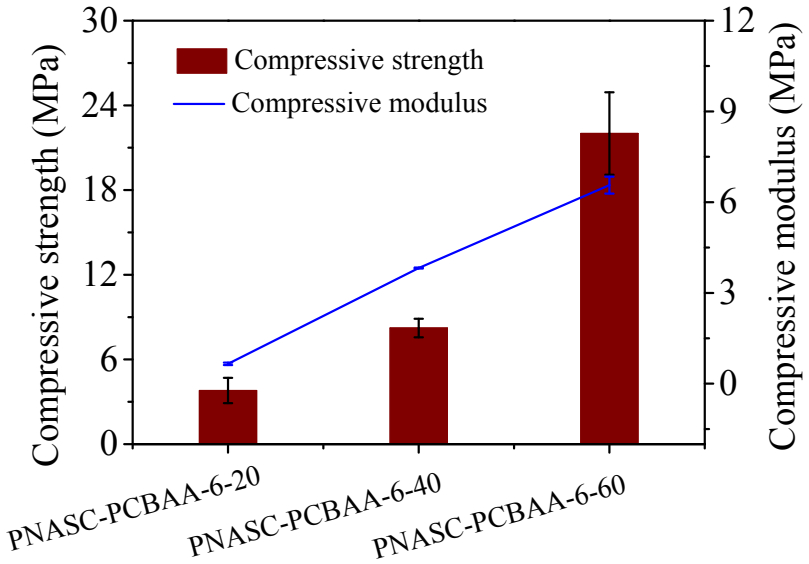

Figure S13. Compressive strength and modulus of PNASC-PCBAA-6-m hydrogels. (n=3)

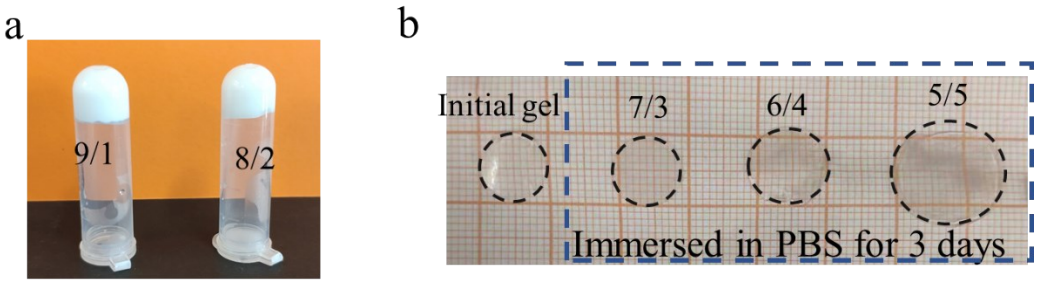

Figure S14. Aqueous solution of NASC and CBAA (mass ratio of NASC/CBAA: 9/1, 8/2, 7/3, 6/4, 5/5; the total concentration of NASC and CBAA was fixed at 20%, w/v%) was photopolymerized for 40 min. (a) Macrophase separation was observed when the ratios of NASC/CBAA were 9/1 and 8/2 due to the relative hydrophobicity of PNASC. (b) The transparent gels were obtained when the ratio of NASC/CBAA exceeded 7/3, and the swelling degree was increased with decrease of NASC.

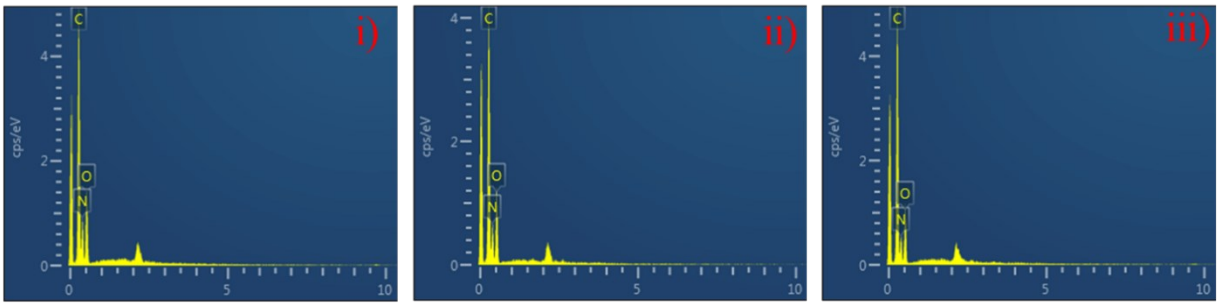

Figure S15. EDS analysis of PNASC-30 (i), PNASC-37.5-PCBAA-8.5 (ii), PNASC-PCBAA-6-40 (iii) hydrogels.

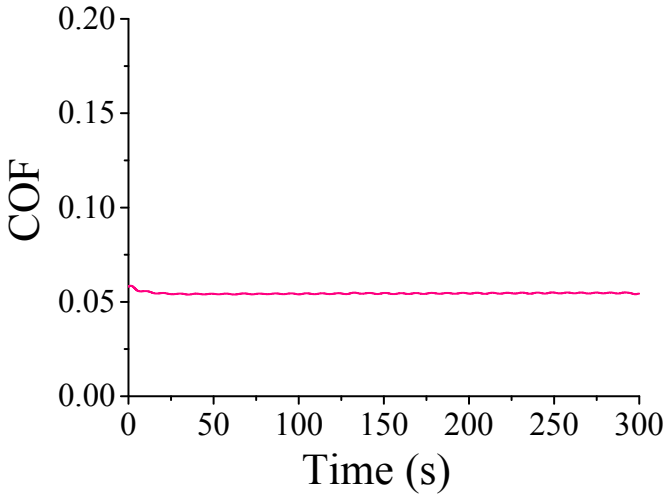

Figure S16. Variation in COF of PNASC-PCBAA-6-40 hydrogels as a function of immersion time in deionized water for 2 months.

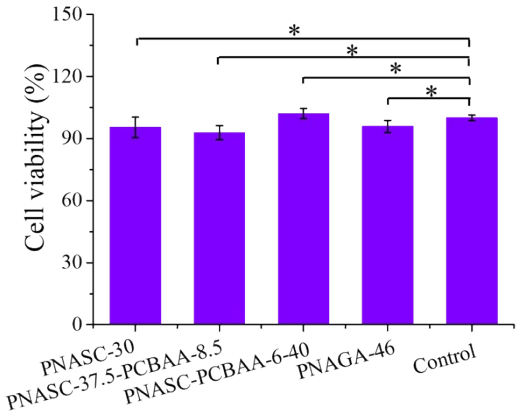

Figure S17. Cytotoxicity results (represented by percentage cell viability) of PNASC-30, PNASC-37.5-PCBAA-8.5, PNASC-PCBAA-6-40, PNAGA-46 hydrogels. (n=5)

Figure S18. A digital photo showing that the soluble PNASC-PCBAA-6-60 ink at an elevated temperature could not transform back into a homogenous gelling state after cooled down to room temperature (the white precipitate was formed as the temperature decreased).

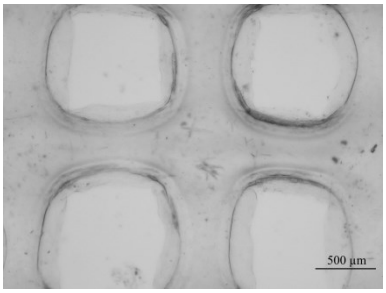

Figure S19. Microstructure of printed hydrogel scaffold measured by Inverted fluorescence microscope.

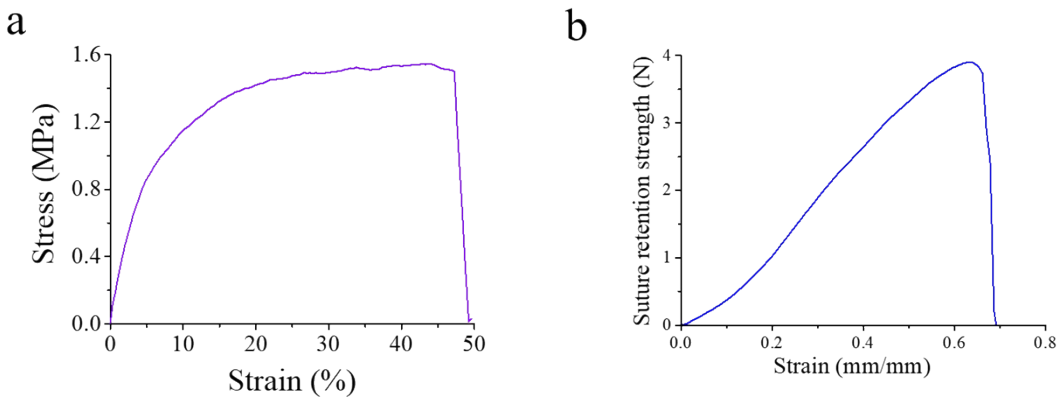

Figure S20. (a) Tensile stress-strain curve of printed single microfiber curve. (b) Suture retention strength of printed PNASC-PCBAA-6-40 meniscus as a function of strain.

Movie S1. 3D printing a triangle using a 3D printer.

Movie S2. Meniscectomy is carried out and then hydrogel scaffold is implanted into knee joint of rabbit.

References

1 C. Fan, B. Liu, Z. Xu, C. Cui, T. Wu, Y. Yang, D. Zhang, M. Xiao, Z. Zhang, W. Liu, *Mater. Horiz.*, 2020, **7**, 1160.

2 H. Wang, Y. Wu, C. Cui, J. Yang, W. Liu, *Adv. Sci.*, 2018, **5**, 1800711.

3 Y. Wang, L. Cheng, S. Wen, S. Zhou, Z. Wang, L. Deng, H.-Q. Mao, W. Cui, H. Zhang, *Nano Lett.*, 2020, **20**, 6420.

4 H. Li, H. Wang, D. Zhang, Z. Xu, W. Liu, *Polymer*, 2018, **153**, 193.